Biomaterials 35 (2014) 4035–4045

Contents lists available at ScienceDirect

Biomaterials

journal homepage: www.elsevier.com/locate/biomaterials

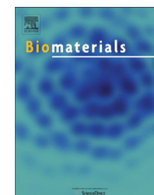

Peripheral nerve morphogenesis induced by scaffold micropatterning

Federica Cerri [a,1], Luca Salvatore [b,1], Danish Memon [c], Filippo Martinelli Boneschi [a], Marta Madaghiele [b], Paola Brambilla [a], Ubaldo Del Carro [a], Carla Taveggia [a], Nilo Riva [a], Amelia Trimarco [a], Ignazio D. Lopez [a], Giancarlo Comi [a], Stefano Pluchino [c], Gianvito Martino [a], Alessandro Sannino [b,*], Angelo Quattrini [a]

[a] Division of Neuroscience and INSPE, San Raffaele Scientific Institute, via Olgettina 60, 20132 Milan, Italy
[b] Department of Innovation Engineering, University of Lecce, Via per Monteroni, 73100 Lecce, Italy
[c] Department of Clinical Neurosciences, Centre for Brain Repair, University of Cambridge, Robinson Way CB2 0PY, UK

A R T I C L E I N F O

Article history:
Received 6 December 2013
Accepted 26 January 2014
Available online 20 February 2014

Keywords:
Biomaterials
Peripheral nervous system
Nerve regeneration
Medical device

A B S T R A C T

Several bioengineering approaches have been proposed for peripheral nervous system repair, with limited results and still open questions about the underlying molecular mechanisms. We assessed the biological processes that occur after the implantation of collagen scaffold with a peculiar porous microstructure of the wall in a rat sciatic nerve transection model compared to commercial collagen conduits and nerve crush injury using functional, histological and genome wide analyses. We demonstrated that within 60 days, our conduit had been completely substituted by a normal nerve. Gene expression analysis documented a precise sequential regulation of known genes involved in angiogenesis, Schwann cells/axons interactions and myelination, together with a selective modulation of key biological pathways for nerve morphogenesis induced by porous matrices. These data suggest that the scaffold's microstructure profoundly influences cell behaviors and creates an instructive micro-environment to enhance nerve morphogenesis that can be exploited to improve recovery and understand the molecular differences between repair and regeneration.

© 2014 Elsevier Ltd. All rights reserved.

1. Introduction

Unlike the central nervous system (CNS), peripheral nervous system (PNS) has an innate capacity to regenerate itself in order to fill injuries below a critical size and only if Schwann cell basal lamina integrity is maintained. None-the-less, the regenerated fibers have thinner myelin sheaths than those of normal fibers [1], and never show complete functional recovery. Over the last decades much effort has been made to provide biomaterials that could influence cell behavior in order to efficiently repair injured gaps in peripheral nerves, and to increase our understanding in the molecular differences between regeneration in PNS and CNS, and between development and regeneration. Although biomaterials can direct cells growth and influence specific patterns of gene expression (GE) in cell cultures, tissue regeneration *in vivo* is a complex event, involving intrinsic and extrinsic factors that are critical for proper tissue development and function [2].

Several studies have already described tissue engineering paradigms that may induce nerve regeneration using organic [3] or synthetic materials [4]. The use of a tubular construct (conduit) reconnecting proximal and distal stumps of a transected nerve is capable of inducing regeneration *in vivo*, and has been the subject of a large number of investigations that gave different degrees of success [5]. The conduit should protect the site of injury from the infiltration of surrounding cells [6,7], while at the same time should retain a certain degree of porosity allowing diffusion of soluble factors through the tube wall, as well as affecting the migration and organization of myofibroblasts, which are responsible for the undesired synthesis of scar tissue [6]. Thus, the capacity to limit and/or prevent the formation of the contractile capsule of myofibroblasts, as well as a certain grade of permeability are two key factors which must be carefully considered when working at the improvement of the tube wall properties. Moreover, the orientation of the pores has also been shown to play a critical role in its performance [8–10], together with the biodegradation rate of the conduit [11]. Several studies have focused on the fabrication techniques that create a gradient in pore size along the tube wall [12], combining multiple manufacturing methods in order to increase the level of manipulation in scaffold micro-structures [13]. Even

* Corresponding author. Tel.: +39 0832 297259; fax: +39 0832 297240.
E-mail address: alessandro.sannino@unisalento.it (A. Sannino).
[1] Federica Cerri and Luca Salvatore contributed equally to this work.

0142-9612/$ – see front matter © 2014 Elsevier Ltd. All rights reserved.
http://dx.doi.org/10.1016/j.biomaterials.2014.01.069

though an adequate porosity is considered a critical point for the enhanced nerve regeneration [4], conclusive results about the ability of porous conduit to improve regeneration *in vivo* are still lacking [13,14].

Although many studies have investigated the effectiveness of nerve conduits in nerve repair, few data have been collected on the molecular mechanisms underlying nerve regeneration inside the conduits. Moreover, whether biomaterials can recreate the complexity of molecular processes that take place during morphogenesis is still an unsolved question as well as one of the major goals of tissue engineering [2].

We have developed a micro-patterned collagen scaffold (MPCS) obtained by means of low cost spinning technique [15], based on thermodynamic and sedimentation phenomena to control pore size gradient and orientation, without the use of any complex mold. The main purpose of our study was to assess the extent of nerve regeneration induced by novel collagen scaffold and to dissect the biological events that occur inside the conduit in rat sciatic nerve repair *in vivo*. In order to evaluate if and how porous micropatterning might influence nerve regeneration, we performed comparative studies using morphological, functional and gene expression analyses.

2. Materials and methods

Experiments with animals followed protocols approved by the Institutional Animal Care and Use Committees.

2.1. Preparation of scaffolds and surgical procedures

As reported elsewhere [15], micro-patterned collagen scaffolds (MPCS) were prepared starting from a collagen-based slurry, spun in a proper apparatus, frozen in liquid nitrogen and transferred to a freeze-dryer for lyophilization. Two aqueous suspensions differing for the collagen concentration (either 3% or 5% w/v Type-I collagen from bovine dermis, Symatese Biomateriaux) were used, in order to obtain scaffolds with different pore size and pore volume fraction. The two types of scaffolds were referred to as MPCS#1 (3% w/v collagen, high porosity scaffold) and MPCS#2 (5% w/v collagen, low porosity scaffold). After freeze-drying, all the scaffolds were cross-linked via a standard dehydrothermal (DHT) process (121 °C, 30 mmHg, 72 h), to slightly strengthen the collagen network by introducing covalent cross-links among the polypeptide chains. Pore diameters were quantified by scanning electron microscopy images of scaffolds.

The biological properties of the two kinds of scaffolds were preliminarily screened in a rat model of sciatic nerve transection. The two types of MPCS ($3 + 3$ animals for MPCS#1 and #2) were implanted in two-month-old female Sprague–Dawley rats after experimental transection of the sciatic nerve. To implant the scaffolds, rats were anesthetized with chloral hydrate 0.5 g/kg, the sciatic nerve was exposed and a segment was then cut, immediately after the sciatic notch and before distal sciatic nerve branches to leave a gap of about 10-mm after retraction of the ends. The 15-mm conduit was interposed between the proximal and distal stumps and fixed with a single 11-0 nylon suture. Considering the superior cell infiltration into MPCS#1 (high porosity) over MPCS#2 (low porosity), only the former scaffolds were studied further in comparison to commercial collagen conduits-NeuraGen® (CCNG), without any pore size gradient in the wall. Animals were implanted unilaterally with MPCS#1 ($n = 30$) and with CCNG ($n = 24$).

For crush injury, adult rats were anesthetized with chloral hydrate 0.5 g/kg, and crush injury was performed as described [16]. After skin incision, the sciatic nerve was exposed and crushed at distal to the sciatic notch for 20 s with fine forceps previously cooled in dry ice. To identify the site of injury, forceps were previously dropped into vital carbon. The nerve was replaced under the muscle and the incision sutured ($n = 9$).

2.2. Neurophysiological and morphological analyses

To evaluate the degree of regeneration and remyelination after peripheral nerve transection, we performed: (i) longitudinal sciatic nerve conduction studies on rats following implantation of both conduits at 90 and 120 days; (ii) serial morphological studies at different levels on MPCS- and CCNG-implanted rats at 8, 15, 40, 60, 90, 120 days after the implant. The timeline has been selected on the basis of the biological events known to occur during nerve repair process [17]. To study nerve conduction velocity, rats were anesthetized with chloral hydrate 0.5 g/kg and placed under a heating lamp to avoid hypothermia. Sciatic nerve motor conduction velocity was obtained with steel monopolar needle electrodes: a pair of stimulating electrodes was inserted subcutaneously near the nerve at the ankle; and a second pair of electrodes was placed at the sciatic notch, to obtain two distinct sites of stimulation, proximal and distal, along the nerve. Compound motor action potential was recorded with an active electrode inserted in the muscles in the middle of the paw and a reference needle in the skin between the first and second digits. Nerve conduction velocity was evaluated at 90 and 120 days after the implant: 3 animals implanted with MPCS and 3 animals with CCNG were examined at the selected time points and compared to 2 uninjured rats (wt), bilaterally recorded.

For the morphological analysis, animals ($n = 2$ wt rats as control, sciatic nerves were retrieved bilaterally; 5 MPCS- and 4 CCNG-implanted rats per time point) were sacrificed by CO2 inhalation and tissues were removed and fixed with 2% glutaraldehyde in 0.12 M phosphate buffer, postfixed with 1% osmium tetroxide and embedded in Epon (Fluka). Semithin (0.5–1 μm thick) and ultra-thin (100–120 nm thick) sections were obtained and examined by light (Olympus BX51) and electron microscopy (Leo 912 Omega). Sciatic nerves were divided at different levels to ensure the study of the inside of the tube, even after it had been reabsorbed (+2, +4 and +8 mm from the proximal stump). To establish the process of reinnervation at the distal part, together with sciatic nerves, we also investigated the tibial plantar nerves at the paw. Digitalized images of fiber cross-sections were obtained from corresponding levels of the sciatic nerve with a digital camera (Leica DFC300F) using a 100× objective. Morphometry on semithin sections was analyzed with the Leica QWin software (Leica Mycrosystems, Milano, Italy) [18]. The ratio between the mean diameter of an axon and the mean diameter of the fiber including myelin (*g*-ratio), was determined on at least 300 randomly chosen fibers per group (3 animals each MPCS, CCNG and controls) from electron microscopy images [19] taken at different levels inside the conduits and at the peroneal branch of sciatic nerve. Morphometric data differences between control nerves, MPCS and CCC-NG were analyzed by One-Way ANOVA followed by Bonferroni post-hoc test. Statistical significance was considered at $p < 0.05$. All statistical tests were performed using SPSS software (Technologies, Inc., Chicago, IL, USA).

2.3. RNA extraction and gene expression analysis

To investigate the molecular changes in each of the experimental groups, we performed whole genome expression profiling study with Illumina® RatRef-12 Expression Beadchips on MPCS and CCNG-implanted rats at 8, 25 and 40 days post-surgery, compared to sciatic nerve after crush injury and from healthy control rats. Together with MPCS- and CCNG-implanted rats, for gene expression analysis we chose the crush injuries as the control of efficient and accurate regeneration because the basal lamina surrounding the axon/Schwann cells nerve unit is preserved and the integrity of the original paths inside the endoneurium was maintained.

Total RNA was isolated from the sciatic nerves of additional animals, at 8, 25 and 40 days (sciatic nerves were retrieved bilaterally from 2 wt rats as control, from 4 MPCS- and 4 CCNG- unilaterally implanted rats and 3 crushed nerves, for each time point) using the RNeasy kit (Qiagen). RNA was quantified using the Nanodrop-2000 spectrophotometer (Celbio) and Agilent 2100 Bioanalyzer was used to assess RNA integrity. For genome expression (GE) profiling study we used Illumina® RatRef-12 Expression Beadchips. Each individual array on the chip targets more than 21,000 transcripts selected primarily from the NCBI RefSeq database (Release 16) and in minor part from the UniGene database. Total RNA (500 ng) was reverse transcribed into cRNA and biotin-UTP labeled using the Illumina TotalPrep RNA Amplification Kit (Ambion). We quantified the cRNA with three replicate measurements using Nanodrop-2000 spectrophotometer. cRNA (750 ng) in 11 μl (150 ng/μl) were hybridized to the BeadChip Array at 58 °C overnight. The fluorescent signal was developed through a streptavidin-Cy3 staining step. BeadChips were imaged using the Illumina® BeadArray Reader, a two-channel 0.8 μm resolution confocal laser scanner. The software Illumina® GenomeStudio (2010.1) was used to assess fluorescent hybridization signals and the system quality controls, such as biological specimen, hybridization, signal generation and negative controls. Each sample was tested in technical and biological replicates, and the mean correlation coefficient value of technical replicates was 0.991 (SD: 0.004) and of the biological ones was 0.953 (SD: 0.03). Sample clustering analysis based on the absolute correlation metric parameter was performed. The graphical representation of the dendrogram further supported the technical validity of the data.

Initial pre-processing and variance stabilizing normalization of Bead summary data was done using Lumi package [20] in R. The normalized expression values of samples were used to identify differentially expressed genes at different time points of the experiments.

Genes were classified as differentially expressed based on a fold change with a cutoff of 2.0 and adjusted *p* value less than 0.01 to maintain a low false discovery rate. Log fold change and moderated *t*-statistics were determined based on multiple linear models built using Limma package [21] in Bioconductor. The gene ontology/biological pathway enrichment analysis was done using DAVID [22,23] and Gene Ontology database [24]. Functional annotation clustering was performed for enriched biological processes at gene ontology level 5 and representative biological process from each cluster was selected. The gene co-expression networks were built from Pearson correlation coefficients between genes with a hard threshold of 0.95 and visualized in Cytoscape tool [25]. The over-represented transcription factor binding sites in co-regulated genes, were obtained from cREMaG database [26].

2.4. Quantitative real-time PCR analysis

Differential expression of MBP, P0 and GFAP at 25 days post-surgery was validated by quantitative Real Time polymerase chain reaction (qRT-PCR). In C1000

Download English Version:

https://daneshyari.com/en/article/10228040

Download Persian Version:

https://daneshyari.com/article/10228040

Daneshyari.com